

## O-Atom Yields from Microwave Discharges in N<sub>2</sub>O/Ar Mixtures

Lawrence G. Piper\* and Wilson T. Rawlins

Physical Sciences Inc., Research Park, Andover, Massachusetts 01810 (Received: June 24, 1985)

We have studied the products of Ar/N<sub>2</sub>O microwave discharges to determine their fitness as sources of atomic oxygen in discharge-flow reactors. For N<sub>2</sub>O feed rates below 10 to 20 μmol s<sup>-1</sup>, the discharge converts about 75% of the N<sub>2</sub>O to atomic oxygen and, in addition, produces small quantities of atomic nitrogen, generally less than 10% of the O-atom product. At higher N<sub>2</sub>O feed rates the O-atom production efficiency decreases, and some nitric oxide accompanies the O atoms out of the discharge. At intermediate N<sub>2</sub>O feed rates, only atomic oxygen is observed, and neither N nor NO leaves the discharge. The exact point at which this occurs is a function of the discharge power and the Ar/N<sub>2</sub>O mixing ratio. Adding molecular nitrogen to the discharge eliminates any NO product, but at the penalty of a slightly reduced O-atom production efficiency. Atomic oxygen flows in excess of 20 μmol s<sup>-1</sup> are produced at pressures near 1 torr and discharge powers of only 30 W. In kinetic modeling of the discharge chemistry, we can account for the experimental observations only if the electron-impact dissociation of the N<sub>2</sub>O in the discharge proceeds through a spin-forbidden channel to produce O(<sup>3</sup>P). In addition, the model indicates that about 10–20% of the N<sub>2</sub>O dissociations result from collisions between metastable argon atoms in the discharge and N<sub>2</sub>O.

### Introduction

Atomic oxygen sources for flow reactors take a variety of forms, and each has its own particular strengths and weaknesses. The simplest technique for making atomic oxygen is to dissociate molecular oxygen, usually in some form of discharge, the 2.45-GHz microwave discharge being most common.<sup>1</sup> These sources are somewhat limited in overall yield and generally produce large quantities of accompanying electronically excited metastable singlet molecular oxygen, O<sub>2</sub>(a<sup>1</sup>Δ<sub>g</sub>, b<sup>1</sup>Σ<sub>g</sub><sup>+</sup>).<sup>2-5</sup> In pure molecular oxygen the dissociation efficiency is generally only a few percent.<sup>5</sup> If the oxygen is highly diluted in a rare gas buffer such as argon or helium, dissociation efficiencies can exceed 50%,<sup>2,6</sup> but due to the large dilution, the overall atomic oxygen yield is still low.

The other major technique is to exchange O atoms for N atoms by titration with NO:<sup>7</sup>



This technique has the advantage that the absolute flow rates will be equal to the flow rate of the nitric oxide added, provided atomic nitrogen is in excess. Even in this instance, if significant O-atom recombination occurs, a large fraction of the molecular oxygen formed will be O<sub>2</sub>(a<sup>1</sup>Δ<sub>g</sub>).<sup>8</sup> The yields of atomic nitrogen from conventional discharge sources are generally even lower than those from oxygen discharges, so the maximum O-atom flow rates again are limited.

The thermal decomposition of O<sub>2</sub>, O<sub>3</sub>, or N<sub>2</sub>O in contact with a Nernst glower is also useful for certain applications.<sup>9,10</sup> The claims for the lack of reactive-impurity production by this technique conflict and yields are small, being limited to atomic-oxygen flow rates of less than 1 μmol s<sup>-1</sup>.<sup>9</sup>

Photolysis of molecular oxygen or some other oxygen-donating species with vacuum ultraviolet laser pulses provides a potentially very clean source of atomic oxygen.<sup>11</sup> Producing radially and axially uniform number densities of O atoms in the flow tube, however, requires extreme care. In addition, current laser development limits the technique to atomic-oxygen flow rates on

the order of 0.1 μmol s<sup>-1</sup> or less.

Several years ago, Ung reported that microwave discharges through mixtures of Ar/N<sub>2</sub>O/N<sub>2</sub> would produce significant quantities of atomic oxygen, free from molecular oxygen.<sup>12</sup> He deduced atomic-oxygen production rates in N<sub>2</sub>O discharges to be an order of magnitude greater than he could obtain using a molecular-oxygen discharge operating under the same conditions. His measured yields were not large, a maximum O-atom flow rate of 0.5 μmol s<sup>-1</sup>, but the atomic oxygen his discharge produced clearly suffered severe depletion by recombination in the flow region between the discharge and the detector.

Intrigued by Ung's results, and desiring a technique to produce relatively large flows of atomic oxygen without large accompanying flows of molecular oxygen, we decided to investigate further the characteristics of Ar/N<sub>2</sub>O discharges. We determined number densities of atomic-oxygen and either atomic-nitrogen or nitric oxide products in a discharge-flow reactor from measurements of the air afterglow intensity<sup>13,14</sup> as a function of the number density of nitric oxide injected downstream of the discharge. Our results will not support Ung's claim that oxygen-atom production is an order of magnitude more efficient when N<sub>2</sub>O is used as the discharge gas as opposed to molecular oxygen. However, we do find that Ar/N<sub>2</sub>O discharges produce large flow rates of atomic oxygen and that, furthermore, under certain conditions negligible flow rates of atomic nitrogen or nitric oxide accompany the atomic-oxygen flow.

In trying to rationalize our experimental observations with a kinetic model, we were surprised to discover that the spin-forbidden pathway for electron-impact dissociation of N<sub>2</sub>O to produce O(<sup>3</sup>P) must dominate the more endoergic but spin-allowed channel which produces O(<sup>1</sup>D). Furthermore, dissociation of N<sub>2</sub>O by metastable argon atoms in the discharge also appears to be an important dissociation pathway. We describe the experimental methods, results, and the kinetic analysis in the following sections.

### Experimental Section

**Apparatus.** The apparatus is a modification of one we have used previously in a number of other studies.<sup>15-19</sup> It consists of

(1) C. J. Howard, *J. Phys. Chem.*, **83**, 3 (1979).  
 (2) L. Elias, E. A. Ogryzlo, and H. I. Schiff, *Can. J. Chem.*, **37**, 1680 (1959).  
 (3) A. Mathias and H. I. Schiff, *Discuss. Faraday Soc.*, **37**, 38 (1964).  
 (4) R. E. March, S. G. Furnival, and H. I. Schiff, *Photochem. Photobiol.*, **4**, 971 (1965).  
 (5) T. J. Cook and T. A. Miller, *Chem. Phys. Lett.*, **25**, 396 (1974).  
 (6) L. G. Piper, unpublished results.  
 (7) F. Kaufman and J. R. Kelso, *Symp. (Int.) Combust.*, [Proc.], **7th**, 1958, 53 (1959).  
 (8) G. Black and T. G. Slanger, *J. Chem. Phys.*, **74**, 6517 (1981).  
 (9) O. R. Lundell, R. D. Ketcheson, and H. I. Schiff, *Symp. (Int.) Combust.*, [Proc.], **12th**, 1968, 307 (1969).  
 (10) J. L. McCrumb and F. Kaufman, *J. Chem. Phys.*, **57**, 1270 (1972).  
 (11) W. T. Rawlins, L. G. Piper, G. E. Caledonia, and B. D. Green, "COHISE Research," Physical Science Inc., Andover, MA, 1981, report PSI TR-298. Available from the authors upon request.

(12) A. Y. M. Ung, *Chem. Phys. Lett.*, **32**, 351 (1975).  
 (13) F. Kaufman, *Proc. R. Soc. London, Ser. A*, **247**, 123 (1958).  
 (14) F. Kaufman, "Chemiluminescence and Bioluminescence", M. J. Cormier, D. M. Hercules, and J. Lee, Eds.; Plenum: New York, 1973, pp 83-100.  
 (15) L. G. Piper, G. E. Caledonia, and J. P. Kennealy, *J. Chem. Phys.*, **74**, 2888 (1981).  
 (16) L. G. Piper, G. E. Caledonia, and J. P. Kennealy, *J. Chem. Phys.*, **75**, 2847 (1981).  
 (17) L. G. Piper, *J. Chem. Phys.*, **77**, 2373 (1982).  
 (18) W. T. Rawlins and L. G. Piper, *Proc. Soc. Photo-Opt. Instrum. Eng.*, **279**, 58 (1981).  
 (19) L. G. Piper, A. A. Clyne, and P. B. Monkhouse, *J. Chem. Soc., Faraday Trans. 2*, **78**, 1373 (1982).

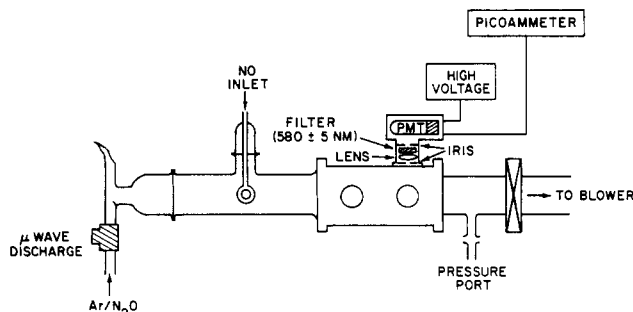


Figure 1. Flow apparatus for Ar/N<sub>2</sub>O discharge experiments.

a 2-in. flow tube pumped by a Leybold-Heraeus Roots blower/forepump combination capable of producing linear velocities up to  $3 \times 10^3$  cm s<sup>-1</sup> at pressures of 1 torr. The flow-tube design is modular (see Figure 1), with separate source, reaction, and detection sections which clamp together with O-ring joints. The detection region is a rectangular stainless-steel block bored out internally to a 2-in. circular cross section and coated with Teflon (DuPont Poly TFE No. 852-201) to retard surface recombination of atoms.<sup>20</sup> The surface was primed with black primer prior to the Teflon coating to reduce scattered light inside the block. Two viewing positions consisting of four circular ports each on the four faces of the block are separated by a distance of 7.5 cm. The circular ports, all of which contain MgF<sub>2</sub> windows, can accommodate vacuum ultraviolet resonance lamps, monochromator interfaces, laser delivery side arms, or, in the case of these studies, a spatially filtered photomultiplier/interference filter combination.

The optical train of the filtered photomultiplier consists of two circular apertures and a 1-in. diameter *f*/1 lens which was 2 in. away from both the center of the flow tube and the photocathode of the photomultiplier. The apertures reduced scattered light from the discharge by a factor of 20. The interference filter in front of the photomultiplier is centered at 580 nm and has a full-width-at-half-maximum band pass of 10 nm. This wavelength is near the peak of the emission from the  $\Delta v = 4$  sequence of the nitrogen first-positive bands when they are excited by atomic nitrogen recombination<sup>21</sup> and also is near the peak of the air-afterglow intensity distribution.<sup>22,23</sup> In addition, this band pass is insensitive to chemiluminescence from the nitric oxide/ozone system which has a short wavelength cutoff of 600 nm<sup>24</sup> and eliminates the strong argon lines scattered from the discharge, most of which are to the red of 700 nm.

A picoammeter (Keithley 417S)/strip-chart recorder (Heath SR 205) combination amplifies and displays the photomultiplier (HTV R955) output. In several experiments a 0.5-m monochromator/thermoelectrically cooled photomultiplier (EMI 9659QA)/photon-counting rate meter (PARC 1105) combination obtained the chemiluminescence spectra in the flow tube between 185 and 800 nm under a variety of conditions to verify the interpretation of the measurements using the filtered photomultiplier.

Flows of argon, nitrous oxide, and, in some cases, nitrogen pass through a 12-mm o.d. Pyrex tube surrounded by a McCarroll microwave-discharge cavity<sup>25</sup> before entering the main flow tube. Nitric oxide in a substantial flow of helium ( $\approx 7\%$  of the total flow) joins the discharge gases in the main section of the flow tube through an injector fabricated from a 1-in.-diameter loop of 2-mm o.d. polyethylene containing a large number of small holes around both its inner and outer perimeters. The helium flow out of the injector gives injected gases a significant velocity as they enter the main flow, thus aiding their mixing.

Mass-flow meters monitor the flow rates of argon and nitrogen, rotameters measure those of nitrous oxide and helium, and

measurement of the rate of increase in pressure with time in a calibrated volume determines the flow rate of nitric oxide. All flow meters were calibrated by measuring rates of increase of pressure with time into 6.5- or 12-L flasks, using appropriate differential pressure transducers (Validyne DP-15) which had themselves been calibrated with silicon oil or mercury manometers. Typically the flow rates for argon, nitrous oxide, and helium were 1400, 0–100, and 120  $\mu\text{mol s}^{-1}$ , respectively, the total pressure was 1.25 torr, and the flow velocity was 1150 cm s<sup>-1</sup>.

The argon and nitrogen flow through molecular-sieve traps to remove water and carbon dioxide prior to entry into the flow reactor, while the helium flows through the injector straight from the cylinder. Most experiments used nitrous oxide (>99.0%) straight from the cylinder without further purification. The major impurity in nitrous oxide is air.<sup>26</sup> We tried removing any air from one lecture bottle of nitrous oxide by freezing the contents of the bottle with liquid nitrogen and then pumping on it until the pressure was below 1 mtorr. No volatile residue remained after a few cycles of thawing, refreezing, and pumping. Experiments with nitrous oxide purified in this manner gave results identical with those in which the nitrous oxide was used straight from the cylinder.

Nitric oxide was purified by flowing it slowly at atmospheric pressure and room temperature through an Ascarite trap and then through a trap immersed in a liquid nitrogen/methanol slush bath (175 K). It was stored in a 5-L bulb. Final nitric oxide purification involved several freeze-pump-thaw cycles of the gas in the storage bulb. The Ascarite trap previously had been baked overnight under vacuum.

*Determination of O and N or NO Number Densities by Air-Afterglow Measurements.* Mixtures of atomic oxygen and nitric oxide emit a continuum radiation, called the air afterglow, which extends from 375 nm to beyond 3000 nm.<sup>13,14,22,23,27–31</sup> The intensity of this emission is directly proportional to the product of the number densities of atomic oxygen and nitric oxide,<sup>13</sup> and independent of pressure of bath gas, at least at pressures above about 0.2 torr.<sup>14</sup> Thus, the emission intensity of the air afterglow is

$$I_{O/NO} = \kappa(\lambda)[O][NO] \quad (2)$$

where  $\kappa(\lambda)$  is a calibration constant specific to the particular viewing geometry and incorporates such things as detection system efficiency, the size of the observation volume, and the absolute air-afterglow rate coefficient.  $\kappa$  is a function of wavelength both through the detection system's spectral response as well as through the wavelength variation of the air-afterglow rate coefficient. We have described elsewhere in great detail how to determine  $\kappa$ .<sup>11,16,32</sup>

The experimental measurements involved monitoring the air-afterglow intensity at three to five different number densities of added nitric oxide. (An experimental data set is illustrated in supplementary Figure S1. See paragraph at end of text regarding supplementary material.) The atomic-oxygen number density is given by the ratio of the slope of the  $I_{O/NO}$  vs.  $[NO]_{\text{added}}$  plot to the calibration constant,  $\kappa$ . An intercept of the  $I_{O/NO}$  vs.  $[NO]$  line on the ordinate indicates that nitric oxide is an N<sub>2</sub>O-discharge product along with the atomic oxygen, and the number density of this product NO is the ratio of the intercept and slope of the  $I_{O/NO}$  vs.  $[NO]$  line. An intercept on the abscissa indicates that nitrogen atoms, produced in the N<sub>2</sub>O discharge along with the atomic oxygen, consumed some of the added NO (reaction 1).

(26) D. Manson, Matheson Gas Co., Gloucester, MA. Private communication to L. G. Piper.

(27) M. Vanpee, K. D. Hill, and W. R. Kineyko, *AIAA J.*, **9**, 135 (1971)

(28) M. F. Golde, A. E. Roche, and F. Kaufman, *J. Chem. Phys.*, **59**, 3953 (1973).

(29) D. Golomb and J. H. Brown, *J. Chem. Phys.*, **63**, 5246 (1975).

(30) G. A. Woolsey, P. H. Lee, and W. D. Slafer, *J. Chem. Phys.*, **67**, 1220 (1977).

(31) A. M. Privilov and L. G. Smirnova, *Kinet. Catal.*, **19**, 202 (1978).

(32) L. G. Piper, W. T. Rawlins, and R. A. Armstrong, "O-Atom Yields from Microwave Discharges in N<sub>2</sub>O/Ar Mixtures". Air Force Geophysics Laboratory, Hanscom AFB, MA, 1983, report AFGL-TR-83-0031. Available from the authors on request.

(20) H. C. Berg and D. Kleppner, *Rev. Sci. Instrum.*, **33**, 248 (1962).

(21) M. F. Golde and B. A. Thrush, *Rep. Prog. Phys.*, **36**, 1285 (1973).

(22) A. Fontijn, C. B. Meyer, and H. I. Schiff, *J. Chem. Phys.*, **40**, 64 (1964).

(23) M. Sutoh, Y. Morioka, and M. Nakamura, *J. Chem. Phys.*, **72**, 20 (1980).

(24) P. N. Clough and B. A. Thrush, *Trans. Faraday Soc.*, **63**, 915 (1967).

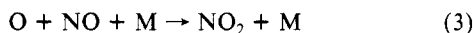
(25) B. McCarroll, *Rev. Sci. Instrum.*, **41**, 279 (1970).

The initial N-atom number density is equal to the added NO number density at the point of intersection of the  $I_{O/NO}$  line and the abscissa. O-atom number densities determined from the slope of such plots must be corrected for the additional atomic oxygen made in the titration of the initial N atoms with the NO. The large rate coefficient for reaction 1<sup>33-35</sup> and the long flow time from the discharge to the observation point ( $\approx 45$  ms) preclude the possibility that both atomic nitrogen and nitric oxide will coexist as far as the detection region.

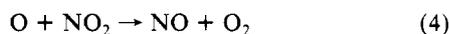
A series of calibrations taken over a period of time established  $\kappa$  to  $\pm 8\%$ . The slopes of the  $I_{O/NO}$  vs.  $[NO]$  plots for the determination of  $[O]$  had standard deviations less than 5%. Thus, the determination of  $[O]$  is in principle accurate to  $\pm 10\%$ .

After determining the O-atom and N-atom or NO number densities, we converted them to flow rates so that we could make reasonable comparisons from one set of conditions to another. This approach affords greater recognition of the similarities and differences between experimental runs. For example, runs with 1400  $\mu\text{mol s}^{-1}$  of argon through the discharge generated approximately the same O- and NO-product flow rates from a given input of  $N_2O$  whether the pressure was 0.52 or 1.25 torr. The number densities of the products from the two experiments, however, differed by a factor of 2.5. Under our base line set of conditions,  $F_{Ar} \approx 1400 \mu\text{mol s}^{-1}$ ,  $F_{He} \approx 115 \mu\text{mol s}^{-1}$ ,  $p \approx 1.2$  torr, and 30 W forward power from the discharge, an atomic-oxygen flow rate of  $20 \mu\text{mol s}^{-1}$  corresponds to an O-atom number density of about  $5 \times 10^{14}$  atoms  $\text{cm}^{-3}$ . In one experiment we produced more than 30 mtorr of atomic oxygen 150-ms downstream from the discharge at a power of only 30 W.

One complication in using the air-afterglow technique to measure O-atom number densities is the slow removal of atomic oxygen in a three-body recombination reaction with NO:



$$k_3 = 7 \times 10^{-32} \text{ cm}^6 \text{ molecule}^{-2} \text{ s}^{-1} \text{ for } M = \text{Ar}^{36}$$



$$k_4 = 9.5 \times 10^{-12} \text{ cm}^3 \text{ molecule}^{-1} \text{ s}^{-1}^{36}$$

The second reaction is fast and maintains a constant NO number density, while doubling the effective rate at which O is removed in reaction 3. The effect of these reactions is strongest at higher pressures ( $\geq 1.5$  torr), longer mixing times ( $\geq 30$  ms), and large NO number densities ( $\geq 10^{14}$  molecules  $\text{cm}^{-3}$ ). Corrections for this effect were generally less than 5% in the calibration experiments to determine  $\kappa$ . However, in a few of the experimental runs at higher pressures, slower flow velocities, and large product nitric oxide number densities, the corrections were large. The iterative procedure for these corrections is detailed elsewhere.<sup>32</sup>

## Results

**General Observations.** Figure 2 shows how the emission intensity at 580 nm varies with the flow rate of  $N_2O$  through the discharge for several different discharge powers. As the  $N_2O$  flow rate increases from zero, the emission intensity rises to a peak, then drops to zero (see inset), increases again very sharply, and finally levels off at the highest  $N_2O$  flow rates. The color of the chemiluminescence is yellow-orange at low flow rates, changes to a very faint blue near where the 580-nm signal drops to zero, and finally turns grey-green at high  $N_2O$  flow rates. While the observed color variations and the subsequent results of the O, N, and NO number density measurements suggested a fairly obvious interpretation of these observations, we took spectra<sup>32</sup> of the

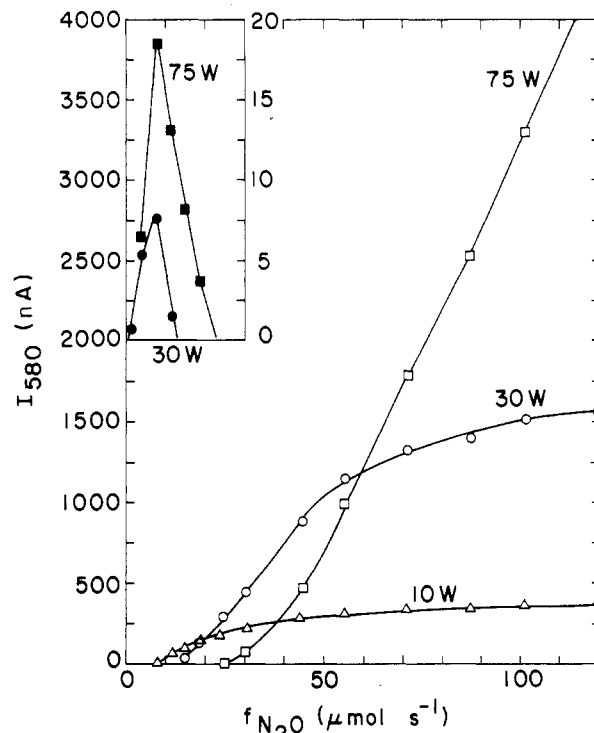


**Figure 2.** Variation in emission intensity at 580 nm from Ar/ $N_2O$  discharge products as a function of  $N_2O$  flow rate. The inset shows intensity variations at low  $N_2O$  flow rates where the signal levels are two orders of magnitude below those at higher  $N_2O$  flow rates.  $f_{Ar} = 1395 \mu\text{mol s}^{-1}$ ,  $p = 1.13$  torr.

emissions in the reactor under several different sets of conditions so that our interpretation would be unequivocal.

The ultraviolet spectrum (available in the supplementary material as Figure S2) was strongest at  $N_2O$  flow rates between those giving the initial small 580-nm intensity peak and the dark point. Prominent spectral features were the NO  $\beta$ -,  $\gamma$ -, and  $\delta$ -bands which result from three-body recombination of O and N atoms.<sup>37,38</sup> For  $N_2O$  additions past those giving the 580-nm dark point, this spectrum is completely extinguished.

The major spectral features between 500 and 800 nm (supplementary material Figure S3), when the  $N_2O$  flow rates are adjusted to give the initial 580-nm intensity peak in the  $I_{580}$  vs.  $F_{N_2O}$  plot, were the nitrogen first-positive ( $B^3\Pi_g - A^3\Sigma_u^+$ ) bands with a vibrational distribution peaked at vibrational levels 10, 11, and 12, characteristic of three-body N-atom recombination.<sup>21</sup> Minor features were the 558-nm line from OI ( $^1S - ^1D$ ) and the  $O_2(b^1\Sigma_g^+ - X^3\Sigma_g^-)$  atmospheric-oxygen band at 762 nm, both of which are excited in three-body O-atom recombination<sup>37,39</sup> and, also in the case of O( $^1S$ ), in the transfer from  $N_2(A^3\Sigma_u^+)$  to O( $^3P$ ).<sup>17</sup> Atomic-nitrogen recombination produces the  $N_2(A)$ .<sup>21</sup>

Adjusting the  $N_2O$  flow rate beyond the dark point in the  $I_{580}$  vs.  $F_{N_2O}$  plot resulted only in the air-afterglow continuum emission which results from recombination of atomic oxygen and nitric oxide and the previously observed atmospheric-oxygen band at 762 nm.

The preceding observations identify atomic nitrogen and atomic oxygen as discharge products at low  $N_2O$  flow rates. At high  $N_2O$  flow rates nitric oxide accompanies the atomic oxygen, and at some intermediate  $N_2O$  flow rate, the discharge produces neither nitric oxide nor atomic nitrogen, only atomic oxygen. Figure 2 shows that this intermediate point where neither N nor NO is made is a function of discharge power, occurring at higher  $N_2O$  flow rates when the discharge power is higher. The initial peak in intensity at 580 nm which is due to atomic-nitrogen recombination is much

(33) D. Husain and N. K. H. Slater, *J. Chem. Soc., Faraday Trans. 2*, **76**, 606 (1980).

(34) J. H. Lee, J. V. Michael, W. A. Payne, and L. J. Stief, *J. Chem. Phys.*, **69**, 3069 (1978).

(35) M. A. A. Clyne and I. S. McDermid, *J. Chem. Soc., Faraday Trans. 1*, **71**, 2189 (1975).

(36) D. L. Baulch, D. D. Drysdale, D. G. Horne, and A. C. Lloyd, "Evaluated Kinetic Data for High Temperature Reaction. II. Homogeneous Gas Phase Reactions of the  $H_2 - N_2 - O_2$  System", Butterworths, London, 1973.

(37) R. A. Young and R. L. Sharpless, *J. Chem. Phys.*, **39**, 1071 (1963).

(38) W. Groth, D. Kley, and U. Schurath, *J. Quant. Spectrosc. Radiat. Transfer*, **11**, 1475 (1971).

(39) G. Slanger and G. Black, *J. Chem. Phys.*, **64**, 3767 (1976).

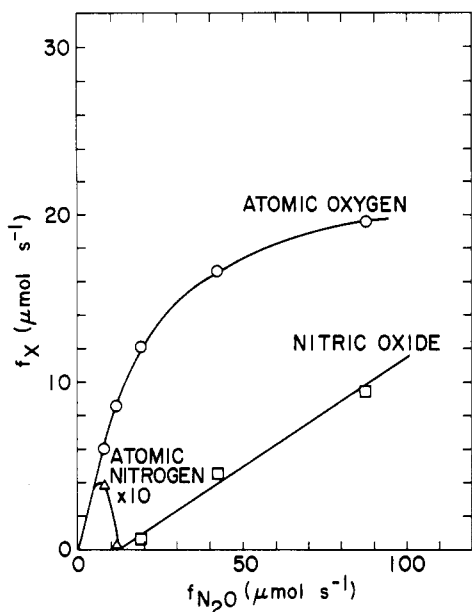


**Figure 3.** The production of O, N, and NO from Ar/N<sub>2</sub>O discharges as a function of N<sub>2</sub>O flow rate. Power = 30 W, pressure = 1.24 torr,  $f_{\text{total}} = 1461 \mu\text{mol s}^{-1}$ .

more intense at higher discharge powers, indicating greater N-atom production rates at higher powers. The dramatic increase in the air-afterglow signal at higher discharge powers that is observed at high N<sub>2</sub>O flow rates shows that the higher-power discharges produce much more O and NO. At low discharge powers the O and NO production reaches a plateau when 25–30% of the available discharge power is consumed dissociating N<sub>2</sub>O.

**Quantitative Observations.** Figure 3 shows how the flow rates of O and N or NO out of the discharge vary with the flow rate of N<sub>2</sub>O into the discharge. At low N<sub>2</sub>O flow rates, the discharge converts approximately 75% of the N<sub>2</sub>O into atomic oxygen. Under similar conditions in our system, Ar/O<sub>2</sub> discharges convert only about 30% of the molecular oxygen to atoms, while Ar/N<sub>2</sub> discharges dissociate only about 5% of the molecular nitrogen.

Atomic-nitrogen yields from the Ar/N<sub>2</sub>O discharges at low flow rates are generally 10% or less than those of atomic oxygen. Nitric oxide production at the higher N<sub>2</sub>O flow rates, on the other hand, approaches that of atomic oxygen under certain conditions. An additional interesting feature is that the product-NO flow rates appear to increase linearly as the N<sub>2</sub>O flow rate through the discharge is increased.

Experiments with different argon flow rates at constant total pressure or constant discharge residence time showed that higher Ar/N<sub>2</sub>O mixing ratios suppress nitric oxide production: the onset of NO formation is delayed to higher N<sub>2</sub>O flow rates, and the efficiency of NO production as a function of N<sub>2</sub>O flow rate is smaller for larger flows of argon through the discharge. At constant argon flow rate, however, nitric oxide formation depends upon neither discharge residence time nor pressure.

A He/N<sub>2</sub>O discharge produces nitric oxide at all N<sub>2</sub>O flow rates and, in addition, is 25–30% less efficient as a source of atomic oxygen than is the Ar/N<sub>2</sub>O discharge (Figure 4). This lower efficiency is consistent with our observations that the fractional O<sub>2</sub> dissociations in He/O<sub>2</sub> discharges are only about 20–25% in our system compared to the  $\approx 30\%$  fractional dissociation in an Ar/O<sub>2</sub> discharge. We discuss the differences between the Ar/N<sub>2</sub>O and He/N<sub>2</sub>O discharges further in the next section.

Adding molecular nitrogen to the discharge suppresses nitric oxide formation, but at the expense of a reduced atomic-oxygen production efficiency (Figure 5). For low initial nitrous oxide flow ( $\lesssim 20 \mu\text{mol s}^{-1}$ ), fairly small flows of N<sub>2</sub> remove all the NO whereas, for high initial nitrous oxide flows ( $\gtrsim 60 \mu\text{mol s}^{-1}$ ), N<sub>2</sub> additions must exceed 30% of the total flow through the discharge to remove the NO.

Increased discharge power enhances significantly atomic-oxygen yields at the higher N<sub>2</sub>O flow rates. At the low N<sub>2</sub>O flow rates,

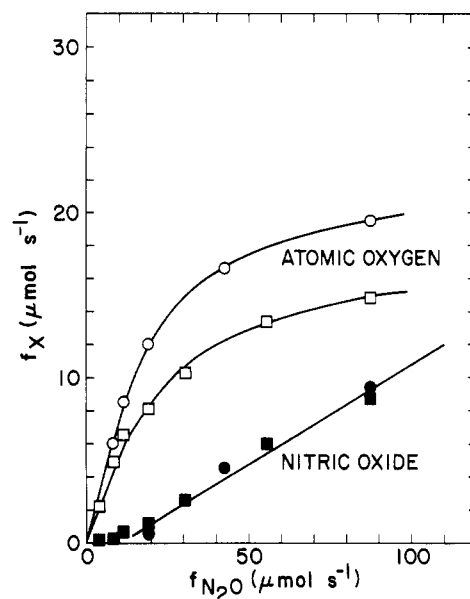


**Figure 4.** The production of O and NO from Ar/N<sub>2</sub>O discharges as a function of N<sub>2</sub>O flow rate for Ar and He buffer gases.  $f_{\text{Ar}} \approx f_{\text{He}} \approx 1475 \mu\text{mol s}^{-1}$ ;  $p = 1.2$  torr; power = 30 W: circles, argon; squares, helium.

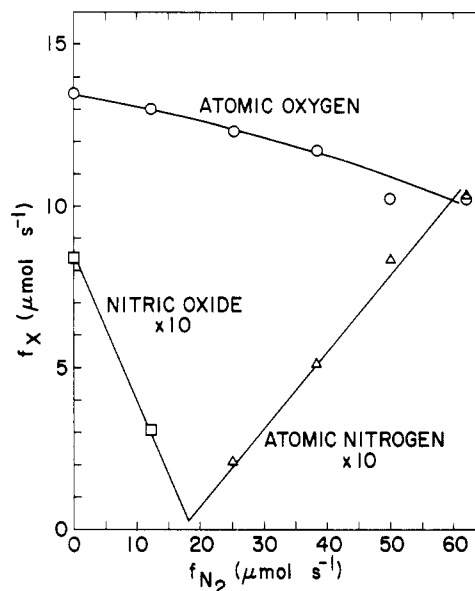


**Figure 5.** Variation in the flow rates of O, N, and NO products from Ar/N<sub>2</sub>/N<sub>2</sub>O discharges as a function of N<sub>2</sub> flow rate.  $f_{\text{Ar}} = 1390 \mu\text{mol s}^{-1}$ ,  $f_{N_2O} = 18.5 \mu\text{mol s}^{-1}$ ,  $p \approx 1.25$  torr, power = 30 W.

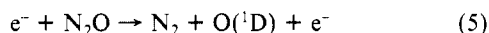
30- and 50-W discharges produce O atoms from N<sub>2</sub>O with equal efficiency. However, at the highest N<sub>2</sub>O flow rate studied, a 50-W discharge produces 30% more atomic oxygen than does a 30-W discharge. The higher power discharge also delays nitric oxide formation to larger N<sub>2</sub>O flows. The above observations are illustrated further in the supplementary material, Figures S4–S10.

### Kinetic Interpretations

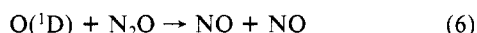
**General Considerations.** To provide a better understanding of the discharge kinetics, we have assembled and exercised a simple kinetic model, assuming typical (and somewhat idealized) discharge properties and surface recombination efficiencies. The model includes the major production and loss terms for each reagent, metastable intermediate, and product which is likely to contribute significantly to the observed results. The resulting rate equations are sufficiently coupled so as to require numerical solution by computer. Kinetic modeling in this context substantiates mechanistic interpretations of the experimental data. It does not determine quantitative rate coefficients or species concentrations, nor is it intended to. However, the results of the

modeling do give useful estimates of the magnitude of concentrations of species not observed directly in the experiments.

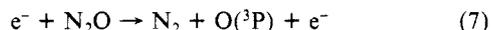
Following Ung,<sup>12</sup> we expected N<sub>2</sub>O decomposition in a microwave discharge would occur primarily via the spin-allowed electron-impact dissociation pathway



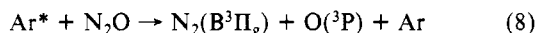
with the O(<sup>1</sup>D) rapidly quenched to O(<sup>3</sup>P) by Ar and wall collisions or converted to NO by reaction with N<sub>2</sub>O:



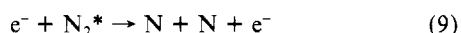
Given the rate coefficients for O(<sup>1</sup>D) removal by N<sub>2</sub>O,<sup>40</sup> N<sub>2</sub>,<sup>40</sup> and Ar<sup>41</sup> and our typical experimental conditions one would expect at least one-third of the O(<sup>1</sup>D) produced in reaction 5 to form NO via reaction 6. This would give about one NO molecule for every two N<sub>2</sub>O molecules destroyed, or roughly equal NO and O(<sup>3</sup>P) yields. This conflicts with our observation of [O] >> [NO]. The coupled nature of the equations, however, precludes reliable estimates of the species production rates in the absence of time-dependent calculations. A further complication of this line of reasoning is its failure to account for N-atom production in the discharge. N formation from electron-impact dissociation of N<sub>2</sub>O, N<sub>2</sub>, or NO should be much too slow to compete with NO formed from reaction 6. The kinetic model confirms that the decomposition of N<sub>2</sub>O by reactions 5 and 6 fails to explain our observed O and NO yields and indicates that the spin-forbidden process



must be the major N<sub>2</sub>O decomposition channel. The dissociation of N<sub>2</sub>O by Ar(<sup>3</sup>P) metastables



appears to be another important pathway for O atom production. Electron-impact dissociation of metastable N<sub>2</sub>, primarily N<sub>2</sub>(A<sup>3</sup>Σ<sub>u</sub><sup>+</sup>) formed by rapid cascade from N<sub>2</sub>(B<sup>3</sup>Π<sub>g</sub>) produced in reaction 8, is an important source of N at low initial N<sub>2</sub>O levels:



NO is formed primarily in reaction 6, the O(<sup>1</sup>D) coming from electron-impact excitation of O(<sup>3</sup>P). The supplementary material details the choice of important reactions in the model and their rate parameters.

**Results of Calculations.** The calculations used a modified predictor-corrector computer code designed to solve numerically "stiff" systems of coupled differential equations. Time-dependent solutions extend 500 μs; typical residence times in our discharges are ≈300 μs. Our calculations indicate that the kinetics are nearly in steady state after ≈200 μs (supplementary material, Figure S11). Figure 6 shows the species concentrations as functions of initial N<sub>2</sub>O level at 300 μs. This represents the neutral gas composition at the exit of the active discharge.

Since the actual measurements of O, N, and NO are made some distance downstream from the discharge, we must correct the predicted concentrations to reflect the completeness of the N plus NO reaction 1 between the discharge exit and the measurement station. Figure 7 compares the final, predicted concentrations of O, N, and NO at the measurement port as functions of [N<sub>2</sub>O]<sub>0</sub> with experimental results obtained under comparable conditions. Figure 7 also indicates predictions for the case where N<sub>2</sub>O dissociation by electrons proceeds entirely via the O(<sup>1</sup>D) product channel (reaction 5). The O(<sup>3</sup>P) case clearly compares very nicely with the observations, while the O(<sup>1</sup>D) case gives too much NO and not enough O. More significantly, the predicted [O]/[NO] ratio is inconsistent with experimental results.

NO formation is overpredicted in the case where reactions 5 and 6 are assumed because at early times, before significant N<sub>2</sub> has built up, N<sub>2</sub>O is the major quenching partner for O(<sup>1</sup>D). In

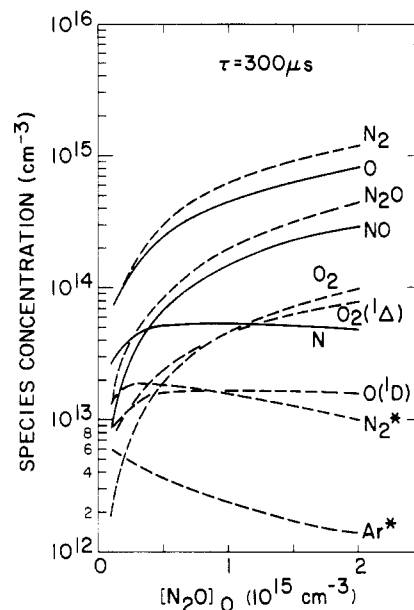


**Figure 6.** Predicted species concentrations at discharge exit (300 μs) as functions of initial N<sub>2</sub>O concentration, using the reaction set in the supplementary material and [Ar] = 2.4 × 10<sup>16</sup> cm<sup>-3</sup>.

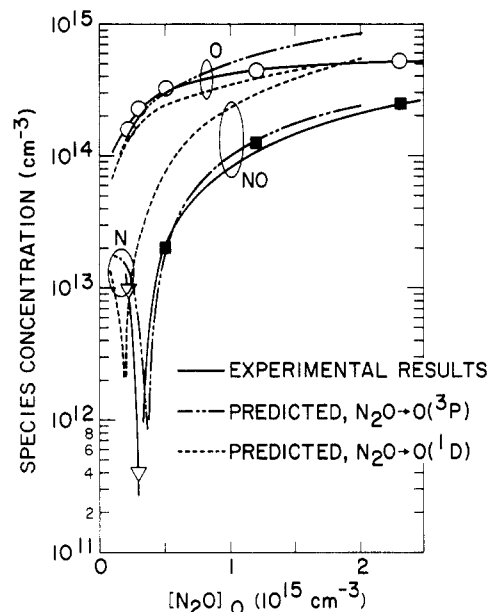


**Figure 7.** Experimental and predicted concentrations of O, N, and NO at the measurement station for an Ar/N<sub>2</sub>O microwave discharge. The solid curve and points are the experimental data from Figure 3.

that case every three N<sub>2</sub>O molecules form two NO molecules but no O(<sup>3</sup>P). As N<sub>2</sub> and NO accumulate, this branching ratio moderates somewhat, but most of the NO has already been formed at this point. Increasing the rate of reaction 5 increases [O] but does not change [NO]. Consuming N<sub>2</sub>O by electrons faster than the O(<sup>1</sup>D) can react with it requires an unreasonably large rate for reaction 5.

Thus direct production of O(<sup>3</sup>P) from N<sub>2</sub>O appears necessary. Reacting N<sub>2</sub>O with Ar\* provides one such source. To obtain [O] > [NO], however, requires an extraordinarily high [Ar\*]. Therefore, we must conclude that, in a microwave discharge, the electron-impact dissociation of N<sub>2</sub>O proceeds primarily, if not entirely, by formation of O(<sup>3</sup>P) in a spin-forbidden process.

Comparison with data obtained for other gas mixtures at similar pressures, flow rates, and discharge powers (i.e., comparable discharge conditions) strengthens our interpretations. Calculations on He/N<sub>2</sub>O mixtures use the same mechanism except, of course, for the reactions involving Ar\*. He\* reactions with N<sub>2</sub>O are unlikely sources of atomic oxygen<sup>32</sup> so we have omitted He\*

(40) L. Lam, D. R. Hastie, B. A. Ridley, and H. I. Schiff, *J. Photochem.*, **15**, 119 (1981).

(41) K. Schofield, *J. Photochem.*, **9**, 55 (1978).

kinetics from our calculations. In accord with the measurements, the calculations predict a 20–30% reduction in O production for He/N<sub>2</sub>O discharges and production of NO at all N<sub>2</sub>O levels (supplementary material, Figure S12). We conclude that the observed reduced O yields result from the absence of the Ar\* + N<sub>2</sub>O reaction and that the continuous production of NO results from the absence of Ar\* which virtually eliminates N<sub>2</sub>\*, and thereby N atoms, the major sink for NO.

Calculations on Ar/N<sub>2</sub>O/N<sub>2</sub> mixtures also predict the general behavior observed in the experiments (supplementary material, Figure S13). In this case, we overpredicted the N production, undoubtedly because the assumed rate coefficient for dissociation of N<sub>2</sub> by electrons is too large. While this process is insignificant for Ar/N<sub>2</sub>O mixtures, it is the major source of N when N<sub>2</sub> is present initially. Furthermore, the addition of such large amounts of N<sub>2</sub> to the discharge will alter significantly the characteristic electron energy distribution and number density and might render kinetic processes involving atomic-nitrogen metastables consequential, although still minor. We considered neither of these factors. The important point, however, is that the kinetic calculations and experimental measurements both show that fairly large amounts of N<sub>2</sub> are required to produce enough N to remove the NO that is formed in reaction 6.

### Summary and Conclusions

The experimental results show that Ar/N<sub>2</sub>O discharges are indeed prolific sources of atomic oxygen. We were able to generate O-atom flows over 20 μmol s<sup>-1</sup> at modest discharge powers. The source is also very efficient, converting about 75% of the nitrous oxide to atomic oxygen at nitrous oxide feed rates less than 10–20 μmol s<sup>-1</sup>. Judicious manipulation of discharge power and the addition of molecular nitrogen to the discharge prevents atomic nitrogen or nitric oxide from accompanying the atomic oxygen

product. The point at which atomic nitrogen and nitric oxide both are absent is indicated readily by the absence of emission at 580 nm, N-atom and O/NO recombination both being strong sources of 580-nm emission.

Kinetic calculations reproduce the experimental results reasonably well under the assumptions that the electron-impact dissociation of N<sub>2</sub>O proceeds through the spin-forbidden channel to produce O(<sup>3</sup>P) and that about 20% of the dissociations result from collisions between metastable argon atoms and N<sub>2</sub>O. The modeling calculations also indicate that perhaps as much as 20% of the nitrous oxide fed to the discharge is undissociated and that the molecular oxygen flow rates out of the discharge are generally an order of magnitude less than those of atomic oxygen. Thus, the argon/nitrous oxide discharge can be a relatively clean source of atomic oxygen with only minor amounts of atomic nitrogen, nitric oxide, or molecular oxygen accompanying the O atoms out of the discharge region, with the two former products being controllable to some extent.

*Acknowledgment.* The Air Force Geophysics Laboratory sponsored this research through Contract No. F19628-82-C-0050. We appreciate insightful discussions with B. D. Green, G. E. Caledonia, and R. H. Krech, all from PSI, and R. A. Armstrong from the Air Force Geophysics Laboratory. We thank H. C. Murphy for his technical assistance.

*Registry No.* NO, 10024-97-2; Ar, 7440-37-1; O, 17778-80-2.

*Supplementary Material Available:* Thirteen additional figures are available to quantify the trends in the data discussed in the text and to illustrate further the comparison between experimental observations and kinetic-model predictions. In addition we provide a table of reactions and rate coefficients used in the model and discuss our reasons for making the choices (19 pages). Ordering information is available on any current masthead page.

## Disproportionation and Combination of Ethyl Radicals in Aqueous Solution

Andreja Bakac\* and James H. Espenson\*

Ames Laboratory and Department of Chemistry, Iowa State University, Ames, Iowa 50011  
(Received: August 5, 1985)

The ratio  $k_{\text{disproportionation}}/k_{\text{combination}}$  ( $k_d/k_c$ ) was determined for ethyl radicals in aqueous solution. Radicals were generated by several independent photochemical and thermal methods: photolysis of (NH<sub>3</sub>)<sub>5</sub>CoO<sub>2</sub>CC<sub>2</sub>H<sub>5</sub><sup>2+</sup>; photolysis of (C<sub>2</sub>H<sub>5</sub>)<sub>2</sub>CO; reduction of ethyl iodide by photochemically generated (CH<sub>3</sub>)<sub>2</sub>CO<sup>-</sup>; reduction of C<sub>2</sub>H<sub>5</sub>C(CH<sub>3</sub>)<sub>2</sub>OOH by V(H<sub>2</sub>O)<sub>6</sub><sup>2+</sup> and by Fe(H<sub>2</sub>O)<sub>6</sub><sup>2+</sup>. The agreement between different methods is good, yielding  $k_d/k_c = 0.35 \pm 0.04$ . The effect of solvent polarity and internal pressure on  $k_d/k_c$  is discussed.

The mechanisms and relative contributions of disproportionation and combination in self-reactions of alkyl radicals have been subjects of interest for some time.<sup>1–6</sup> The effect of solvent on disproportionation/combination ratios ( $k_d/k_c$ ) has been discussed in terms of solvation of the radicals<sup>2,5</sup> and internal pressure<sup>2,4,6a</sup> and viscosity<sup>6b</sup> of solvents.

Our interest in the subject was triggered during our recent investigation of the reduction of alkyl halides by organonickel

complexes, RNi(tmc)<sup>+,7,8</sup> in alkaline aqueous solutions. The kinetics, reaction products, and other observations strongly implied free radical formation. No literature data were available, however, for the value of  $k_d/k_c$  in aqueous solutions with which to compare our findings. We have now determined this ratio for ethyl radicals in water at ~25 °C. By extending the range of solvent polarity and internal pressure examined so far, we hoped to add to the understanding of radical self-reactions in the solution phase.

### Experimental Section

Ethyl radical precursors, [(NH<sub>3</sub>)<sub>5</sub>CoOCC<sub>2</sub>H<sub>5</sub>](ClO<sub>4</sub>)<sub>2</sub> and C<sub>2</sub>H<sub>5</sub>C(CH<sub>3</sub>)<sub>2</sub>OOH, were prepared by literature procedures.<sup>9,10</sup>

(1) Gibian, M. J.; Corley, R. C. *Chem. Rev.* **1973**, *73*, 441 and references therein.

(2) Dixon, P. S.; Stefani, A. P.; Szwarc, M. *J. Am. Chem. Soc.* **1963**, *85*, 2551.

(3) Dixon, P. S.; Stefani, A. P.; Szwarc, M. *J. Am. Chem. Soc.* **1963**, *85*, 3344.

(4) Stefani, A. P. *J. Am. Chem. Soc.* **1968**, *90*, 1694.

(5) Sheldon, R. A.; Kochi, J. K. *J. Am. Chem. Soc.* **1970**, *92*, 4395.

(6) (a) Neuman, R. C., Jr. *J. Org. Chem.* **1972**, *37*, 495. (b) Neuman, R. C., Jr.; Frink, M. E. *J. Org. Chem.* **1983**, *48*, 2430.

(7) Bakac, A.; Espenson, J. H. *J. Am. Chem. Soc.*, in press.

(8) tmc = R,R,S,S-1,4,8,11-tetramethyl-1,4,8,11-tetraazacyclotetradecane.

(9) Jackman, L. M.; Scott, R. M.; Portman, R. H. *Chem. Commun.* **1968**, 1338.